ARCHIVES OF ELECTRICAL ENGINEERING VOL. 67(4), pp. 709–724 (2018)

DOI 10.24425/aee.2018.124735

Study on electric spring control method considering noncritical load voltage constraint

YIXI CHEN, GANG MA, GUCHAO XU, HANG ZHANG, RONG JU

School of Electrical & Automation Engineering, Nanjing Normal University
Wenyuan Road No.1, 210046 Nanjing, China
e-mail: nnumg@njnu.edu.cn

(Received: 02.03.2018, revised: 02.07.2018)

Abstract: With the increasing penetration rate of grid-connected renewable energy generation, the problem of grid voltage excursion becomes an important issue that needs to be solved urgently. As a new type of voltage regulation control method, electric spring (ES) can alleviate the fluctuations of renewable energy output effectively. In this paper, the background and basic principle of the electric spring are introduced firstly. Then, considering the influence of an electric spring on noncritical load voltage, noncritical loads are classified reasonably, and based on the electric spring phasor diagram, the control method to meet the noncritical load voltage constraint is proposed. This control method can meet the requirements of voltage excursions of different kinds of noncritical load, increase the connection capacity of the noncritical load and improve the voltage stabilization capacity of the electric spring. Finally, through the simulation case, the feasibility and validity of electric spring theory and the proposed control method are verified.

Key words: Electric spring, noncritical load, voltage excursion, reactive power compensation

1. Introduction

As the global energy crisis and environmental pollution is worsening, exploitation and utilization of renewable energy has become an effective way to solve the crisis [1, 2]. However, wind, solar and other renewable energy sources have strong intermittence and randomness, and its power generation efficiency changes with time and weather, which will lead to voltage excursions on the electrical load side. As a result, the electrical equipment may not run normally or even be damaged. If some of the critical loads (such as level 1 load) fail, that will lead to serious economic losses and casualties [3, 4].

At present, reactive power compensation technology is widely used for voltage stabilization control. However, this method is centralized compensation, and lacks of flexibility and reliability [5]. And a large number of reactive power output may also lead to line loss increasing. As another

voltage stabilization method for stabilizing renewable power generation and reducing difference between electrical generation and consumption, energy storage devices regain people's attention globally. But this approach will lead to a substantial increase in costs and potential environmental pollution [6, 7].

In 2012, electric spring (ES) technology is proposed, which provides a new method for voltage stabilization of the power grid [8]. The basic principle is similar to the shock absorber. When the grid voltage fluctuates, the ES can ensure that the voltage of the critical load remains stable, and the voltage excursion is transferred to the noncritical load, which can achieve the purpose of stabilizing the grid voltage. The ES is a new voltage regulation control idea. But the study of the ES is still in its infancy. Literature [9] introduces the application of the ES in reducing the installation capacity of energy storage and improving the service life of energy storage equipment. Based on the circuit principle of the ES, literature [10] establishes the dynamic simulation model of the ES. In literature [11], the application of Droop control in multi-ES control in a single power supply line is analyzed. Based on PR control, literature [12] proposed an improved ES control method which can reduce the harmonic caused by the ES. However, the above control methods mainly consider the voltage stability of the critical load, and the excessive voltage excursion will happen to the noncritical load easily. So malfunction or even damage of the noncritical load can be caused. In practical applications, most of the loads have requirements on operating voltage, but the voltage quality requirements of different loads are different. If the noncritical load voltage constraint is ignored, more electrical equipment cannot be allowed to participate in voltage stabilization.

In view of the problems above, combining with the ES's working phasor diagram, an improved ES control method is proposed, which takes the voltage constraint of noncritical load into account. Also, the classification of different noncritical loads is used to ensure the reliable operation of some noncritical load and the improvement of voltage regulation control of the ES at the same time. In this paper, the basic principle of an electric spring is introduced firstly. Then, the noncritical load is classified according to the voltage excursion range. For a load that allows a small range of voltage variations, an ES control method considering the noncritical voltage constraint is proposed by studying the working phasor diagram of the ES under different types of noncritical load and analyzing the voltage relationship between the ES and noncritical load, thus improving the voltage regulation control performance of the ES. Finally, the feasibility and validity of the method are verified by a simulation case, which lays the foundation for the popularization and application of the ES.

2. The working principle of ES

Fig. 1(a) shows the basic circuit diagram of a single ES. From Fig. 1(a), it can be seen that the ES consists of two parts (dashed frame part): a single-phase voltage source PWM inverter and LC low-pass filter [13]. $\boldsymbol{V}_{\mathrm{es}}$ is the voltage across the ES, and $\boldsymbol{I}_{\mathrm{o}}$ is the current flowing through the ES. When the current $\boldsymbol{I}_{\mathrm{o}}$ is 90 degrees ahead of the voltage $\boldsymbol{V}_{\mathrm{es}}$, the ES works in the capacitive mode and provides voltage boosting. When the current $\boldsymbol{I}_{\mathrm{o}}$ 90 degrees lags behind voltage $\boldsymbol{V}_{\mathrm{es}}$, the ES works in the inductive mode and provides voltage reduction. Therefore, the ES can achieve capacitive reactive power and inductive reactive power injection [14]. What needs to be explained

here is that, there is no assumption on $\boldsymbol{V}_{es}$ and it should be sinusoidal, the LC filter is used to eliminate higher harmonic, and the relationship between $\boldsymbol{V}_{es}$ and $\boldsymbol{V}_{s}$ is "$\boldsymbol{V}_{es} + \boldsymbol{V}_{nc} = \boldsymbol{V}_{s}$".

From Fig. 1(b), we can see that, the ES forms a smart load in series with the noncritical load, and the noncritical load consists of a single load or multiple loads [15]. These noncritical loads must be able to withstand large voltage fluctuations and still maintain normal operation. The traditional ES control ignores the working condition of a noncritical load, making a high requirement for the selection of noncritical loads, which leads to most of the electrical loads being unable to be used as noncritical loads to form smart loads with the ES. Hence, the next study is how to meet the voltage constraints of a noncritical load.

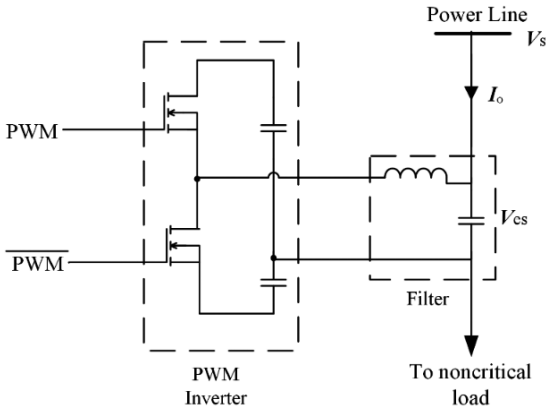

(a)

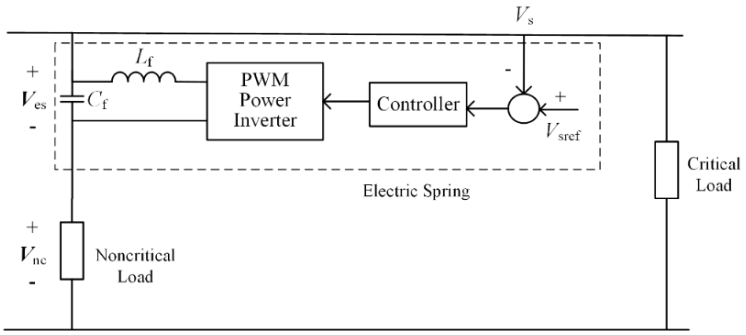

(b)

Fig. 1. Schematic diagram of a typical ES: the basic circuit of ES (a); ES and load (b)

3. The ES control considering voltage constraints of noncritical load

3.1. The classification of noncritical load

Due to the high volatility and unpredictability of renewable energy, the high proportion of noncritical (NC) loads (such as: noncritical load: critical load = 9:1) is essential to insure the

voltage stabilization ability of an ES [10]. But most of the loads cannot be used as noncritical loads due to their own operating voltage limitations. In order to allow more electrical loads to be used as noncritical loads series with the ES, the noncritical load is divided into two categories: class A noncritical load and class B noncritical load. The class A noncritical load is the load which can withstand a certain range of voltage fluctuations, for example, the allowable range of voltage excursion is $a\%$. The class B noncritical load is the load that allows the voltage to fluctuate greatly, which does not have significant damage on itself. Different categories of the noncritical load are installed in series with different ESs. The allowable excursion range of the class A noncritical load can be set according to the actual installation environment. Thus, the improving capacity of the noncritical load and normal operation of the class A noncritical load can be realized at the same time.

In the following section, the relationship between the ES voltage $\boldsymbol{V}_{\mathrm{es}}$ and the noncritical load voltage $\boldsymbol{V}_{\mathrm{o}}$ is analyzed from the perspective of the ES working phasor diagram for two kinds of noncritical load: resistive load and resistive-inductive load. Thus, the voltage excursion constraints of the class A noncritical load can be achieved.

3.2. Resistive load

When the noncritical load is the resistive load, the phasor diagrams of the ES in capacitive mode and inductive mode are shown in Fig. 2.

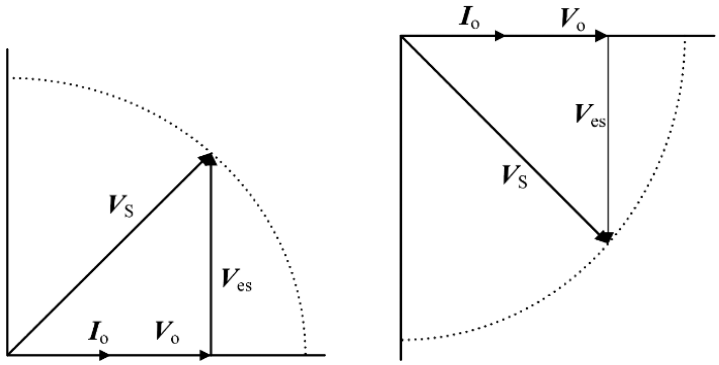

Fig. 2. ES working phasor diagrams when the noncritical load is resistance: inductive mode (a); capacitive mode (b)

From the phasor diagrams of Fig. 2, it can be seen that when the noncritical load is resistive, $\boldsymbol{V}_{\mathrm{o}} < \boldsymbol{V}_{\mathrm{s}}$, and both in the inductive mode and capacitive mode, $\boldsymbol{V}_{\mathrm{es}}$ and $\boldsymbol{V}_{\mathrm{o}}$ satisfy the same relation, which is shown as:

$$V_{\mathrm{s}}^2 = V_{\mathrm{es}}^2 + V_{\mathrm{o}}^2. \tag{1}$$

Solving Equation (1), we can get that (taking positive root):

$$V_{\mathrm{o}} = \sqrt{V_{\mathrm{s}}^2 - V_{\mathrm{es}}^2}. \tag{2}$$

According to Equation (2), the relationship between V_o and V_{es} is shown in Fig. 3 (when $V_s = 220$). It can be seen from Fig. 3 that, when the noncritical load is resistance, V_o deceases monotonically with the increase of V_{es}. Therefore, when the noncritical load rated voltage is V_{ncN}, the allowable excursion range is $a\%$, which is to say the non-critical load voltage lower limit is $(1 - a\%)V_{ncN}$, the maximum value of V_{es} is:

$$V_{es\,max} = \sqrt{V_s^2 - [(1 - a\%)V_{ncN}]}. \tag{3}$$

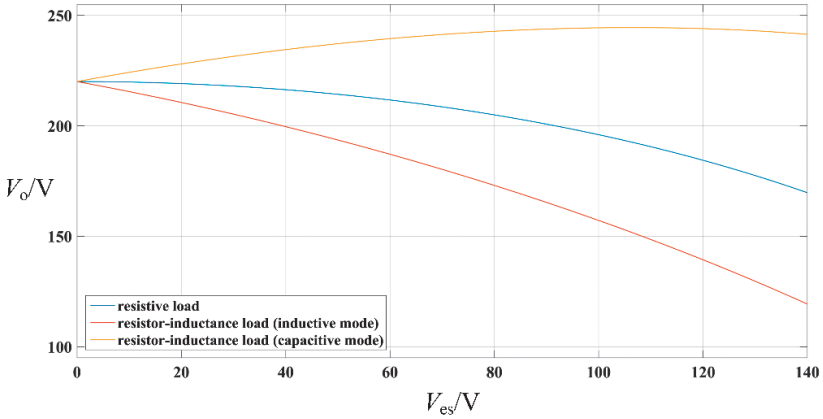

Fig. 3. The relationship between V_{es} and V_o under different type of noncritical load

3.3. Resistive-inductive load

When the noncritical load is the resistive-inductive load, the inductive mode and capacitive mode are analyzed separately.

(1) Inductive mode

When the ES is in the inductive mode, its working phasor diagram is shown in Fig. 4.

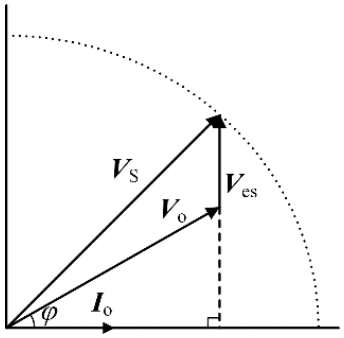

Fig. 4. ES working phasor diagrams when the noncritical load is resistive-inductive (inductive mode)

From the phasor diagram of Fig. 4, it can be seen that $V_o < V_s$, and the relationship between V_{es} and V_o is shown in Equation (4).

$$(V_o \sin\varphi + V_{es})^2 + (V_o \cos\varphi)^2 = V_s^2 . \tag{4}$$

By solving Equation (4), we can get this (taking positive root):

$$V_o = -V_{es} \sin\varphi + \sqrt{V_s^2 - (V_{es} \cos\varphi)^2} . \tag{5}$$

According to Equation (5), the relationship between V_o and V_{es} is shown in Fig. 3 ($V_s = 220$ V, $\cos\varphi = 0.9$). From Fig. 3, it can be found that V_o decreases monotonically with the increase of V_{es}. Therefore, when the noncritical load rated voltage is V_{ncN} and the allowable excursion range is $a\%$, the noncritical load voltage lower limit is $(1 - a\%)V_{ncN}$. The maximum value of V_{es} is:

$$V_{es\,max} = -(1 - a\%)V_{ncN} \sin\varphi + \sqrt{V_s^2 - [(1 - a\%)V_{ncN} \cos\varphi]^2} . \tag{6}$$

(2) Capacitive mode

When the ES is in the capacitive mode, its working phasor diagram is shown in Fig. 5.

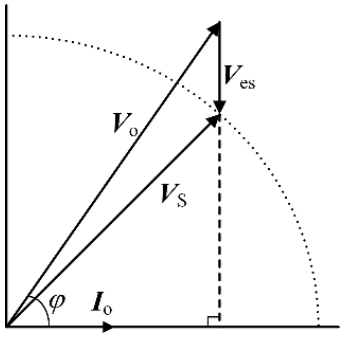

Fig. 5. ES working phasor diagrams when the noncritical load is resistive-inductive (capacitive mode)

From the phasor diagram of Fig. 5, it can be seen that $V_o > V_s$, and the relationship between V_{es} and V_o is shown in Equation (7).

$$(V_o \sin\varphi - V_{es})^2 + (V_o \cos\varphi)^2 = V_s^2 . \tag{7}$$

By solving Equation (7), we can get this:

$$V_o = V_{es} \sin\varphi + \sqrt{V_s^2 - (V_{es} \cos\varphi)^2} , \tag{8}$$

where only positive root is selected, as negative V_o is not conforming to reality in the application.

According to (8), the relationship between V_o and V_{es} is shown in Fig. 3 (when $V_s = 220$ V, $\cos\varphi = 0.9$). From Fig. 3, it can be found that V_o does not monotonically change with V_{es}. It has

maximum value. Therefore, we take the derivative of (8), and the result is shown as follows:

$$V_{\mathrm{o}}' = \sin\varphi - \frac{V_{\mathrm{es}}(\cos\varphi)^2}{\sqrt{V_{\mathrm{s}}^2 - (V_{\mathrm{es}}\cos\varphi)^2}}. \tag{9}$$

Let $V_{\mathrm{o}}' = 0$, we can get that $V_{\mathrm{es}} = V_{\mathrm{s}}\tan\varphi$, then the corresponding V_{o} maximum is:

$$V_{\mathrm{o\,max}} = \frac{V_{\mathrm{s}}}{\cos\varphi}. \tag{10}$$

When the noncritical load rated voltage is V_{ncN}, the allowable excursion range is $a\%$, that is, the noncritical load voltage upper limit is $(1 + a\%)V_{\mathrm{ncN}}$. The maximum value of V_{es} is:

$$V_{\mathrm{es\,max}} = \begin{cases} (1+a\%)V_{\mathrm{ncN}}\sin\varphi - \sqrt{V_{\mathrm{s}}^2 - [(1+a\%)V_{\mathrm{ncN}}\cos\varphi]^2} & (1+a\%)V_{\mathrm{ncN}} < V_{\mathrm{o\,max}} \\ \text{no limit} & (1+a\%)V_{\mathrm{ncN}} > V_{\mathrm{o\,max}} \end{cases}. \tag{11}$$

According to [10], the function relationship between the output voltage V_{es} of the ES and the DC side voltage V_{dc} is shown as follows:

$$V_{\mathrm{es}}(t) = \frac{V_{\mathrm{dc}}}{2}m(t), \tag{12}$$

where $m(t) = M\sin(2\pi 50t + \theta)$ is the modulation index, and $M \in [0, 1]$. Assuming that the DC side voltage maintains the reference value $V_{\mathrm{dc\text{-}ref}}$ without change, the theoretical maximum output of ES RMS voltage is:

$$V_{\mathrm{es\,max}} = \frac{V_{\mathrm{dc\text{-}ref}}}{2\sqrt{2}}. \tag{13}$$

In the synthesis of (3), (6), (11) and (13), we can get the relationship between voltage excursion range $a\%$ and the DC side reference voltage $V_{\mathrm{dc\text{-}ref}}$ under different types of noncritical load:

$$V_{\mathrm{dc\text{-}ref}} = \begin{cases} 2\sqrt{2}\times\sqrt{V_{\mathrm{s}}^2 - [(1-a\%)V_{\mathrm{ncN}}]} \\ \qquad \text{resistance (inductive and capacitive mode)} \\ 2\sqrt{2}\times\left\{-(1-a\%)V_{\mathrm{ncN}}\sin\varphi + \sqrt{V_{\mathrm{s}}^2 - [(1-a\%)V_{\mathrm{ncN}}\cos\varphi]^2}\right\} \\ \qquad \text{resistive-inductive (inductive mode)} \\ 2\sqrt{2}\times\left\{(1+a\%)V_{\mathrm{ncN}}\sin\varphi - \sqrt{V_{\mathrm{s}}^2 - [(1+a\%)V_{\mathrm{ncN}}\cos\varphi]^2}\right\} \\ \qquad \text{resistive-inductive (capacitive mode): } (1+a\%)V_{\mathrm{ncN}} < V_{\mathrm{o\,max}} \\ \text{no limit} \\ \qquad \text{resistive-inductive (capacitive mode): } (1+a\%)V_{\mathrm{ncN}} > V_{\mathrm{o\,max}} \end{cases}. \tag{14}$$

It can be seen from Equation (14) that: by changing the voltage reference value of the ES DC side ($V_{\mathrm{dc\text{-}ref}}$), the adjustment of the output voltage range of the ES can be realized, and it can meet the constraint of the class A noncritical load on voltage excursion. Therefore, considering the noncritical load voltage constraint, the improved ES control structure is shown in Fig. 6.

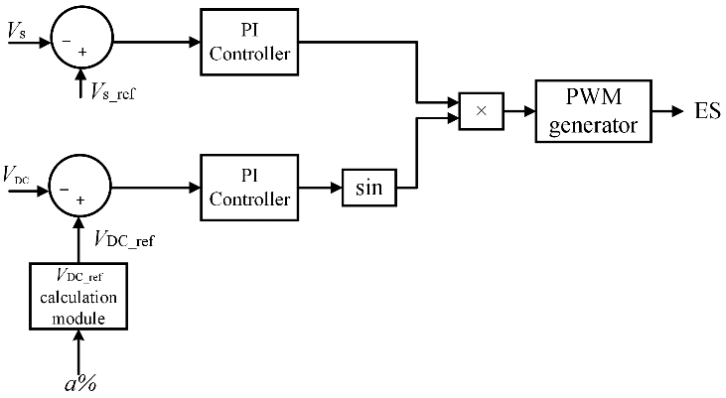

Fig. 6. A schematic diagram of ES control structure considering noncritical load voltage constraint

4. Case simulation and analysis

In this paper, a test model based on MATLAB/Simulink simulation software is built to verify the ES voltage control method, considering the noncritical load voltage constraint. The parameters of the main components are shown in Table 1 and Table 2 [10]. There are 3 kinds of loads: a, b and c with different voltage constraints, where load a $Z_a = 20\ \Omega$, which represents the key electrical equipment, allowing for the voltage excursion amplitude up to 1%; load b $Z_b = 4.5+j2.2\ \Omega$, whose allowable voltage excursion is 7%; load c $Z_c = 9 + j4.4\ \Omega$, which allows a wide range of voltage excursions (without voltage limitation) and does not cause damage to itself. The load rated voltage

Table 1. Power source, line and load simulation parameters

Power source	Capacity (kVA)	100
	Short circuit capacity (kVA)	36
	Transmission impedance ratio (X/R)	10/8
	Voltage level (V)	220
Line impedance	Inductance L (mH/km)	1.24
	Resistance R (Ω/km)	0.11

Table 2. ES simulation parameters

Low-pass filter	Inductance (mH)	5
	Capacitance (μF)	13.2
PI controller	Signal mode	Concrete
	Sampling time T_s (ms)	20
	Proportional coefficient K_p	10
	Integral coefficient K_i	100

of the above three kinds of load are 220 V. In the following, four different load configuration schemes will be analyzed. What needs to be explained here is that, the parameters of model are cited from the laboratory test model in [16], which is applied to conduct the simulation in this paper.

Scheme 1: The ES is not connected to the system.

When the ES does not have access to the system, the loads a, b and c are connected to the system in parallel, which is shown in Fig. 7.

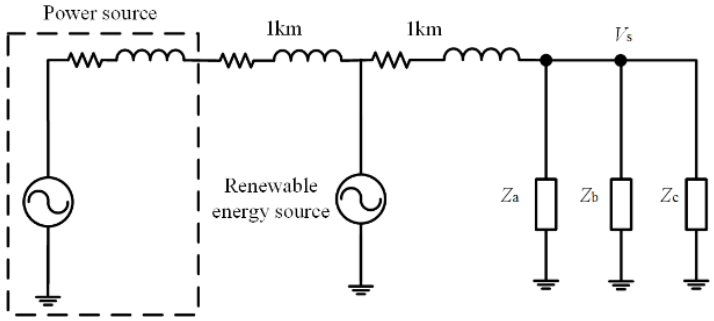

Fig. 7. System diagram of scheme 1

Because the system voltage is mainly affected by the reactive power fluctuation, the simulation of this paper mainly considers the influence of the reactive power fluctuation of the renewable energy on the system voltage. The curve of the reactive power that is absorbed in by the renewable energy source is shown in Fig. 8. When the ES does not have access to the system, the waveform of the system voltage V_s is shown in Fig. 9. At about 5 s, the reactive power absorbed by renewable energy source reaches at the maximum value, and therefore the system voltage V_s drops to the minimum.

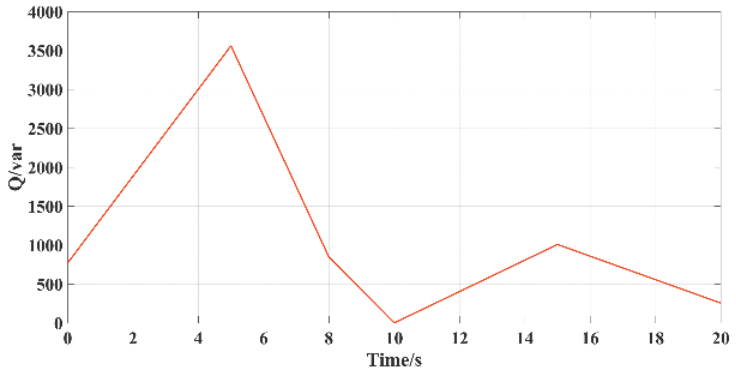

Fig. 8. The reactive power curve of renewable energy source

It can be seen from Fig. 9 that when the ES is not connected, the system voltage V_s continuously changes with the reactive power fluctuation of the renewable energy source, and its maximum

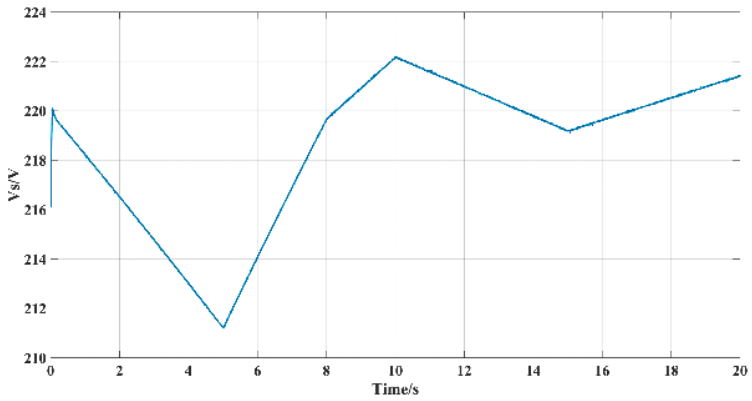

Fig. 9. The system voltage V_s of scheme 1

deviation is up to 9 V (−4.1%, t = 4.6 s), unable to meet the need for the normal work of load a, and may even cause damage to load a. Therefore, Scheme 1 fails to meet the needs of the user.

Scheme 2: The ES is connected to the system. Set load a, b as critical loads, and load c as a noncritical load.

The corresponding system diagram of scheme 2 is shown in Fig. 10, where the ES uses the conventional control method, regardless of the voltage constraint of the noncritical load in series, $V_{\text{dc-ref}}$ = 400 V. The conventional control method was introduced in [10], in which the noncritical load voltage constraint is not considered. The ES starts to run at t = 0 s. The changes of the reactive power of the renewable energy source are the same as that of scheme 1, which has been shown in Fig. 8, then the system simulation waveform is as Fig. 11 shows.

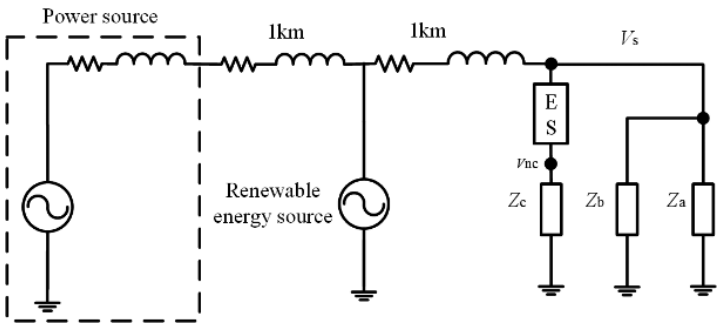

Fig. 10. System diagram of scheme 2

It can be seen from Fig. 11(a) and (b) that when the noncritical load only contains load c, after t = 8 s, the adjustment capacity of the ES reaches the upper limit and loses its adjustment ability. The system voltage still changes with the reactive power of the renewable energy source. The maximum deviation of the system voltage V_s is 3.4 V (+1.54%, t = 10.2 s). Therefore, the normal operation of the important load a, cannot be guaranteed. At the same time, it can be seen from

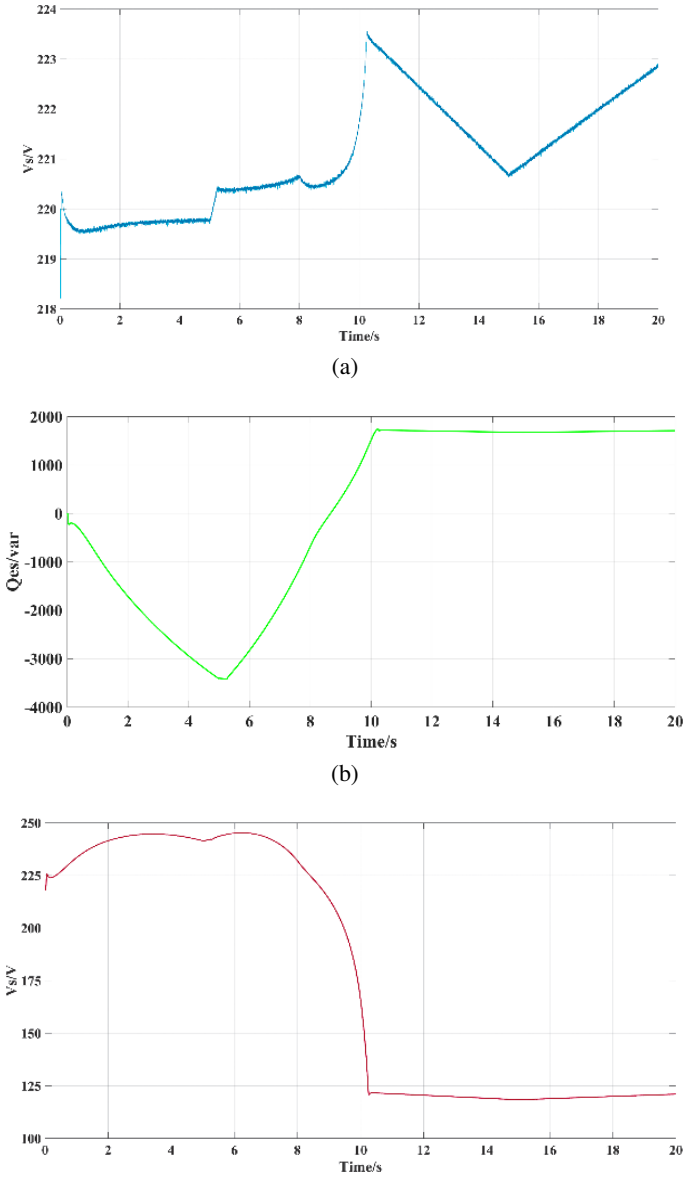

Fig. 11. System simulation waveform of scheme 2: system voltage V_s (a); reactive power of ES Q_{es} (b); noncritical load voltage V_{nc} (c)

the noncritical load voltage V_{nc} waveform that the noncritical load voltage has a large excursion with a maximum value of 245.3 V (+11.5%) and a lowest value of 118.2 V (−46.27%). So, this scheme also cannot meet the needs of the user.

Scheme 3: The ES is connected to the system. Set load a as a critical load, load b and c as noncritical loads.

The corresponding system diagram of scheme 3 has been shown in Fig. 12, where the ES uses the conventional control method, regardless of the voltage constraint of the noncritical load in series, $V_{\text{dc-ref}} = 400$ V. The ES starts to run at $t = 0$ s, the changes of the reactive power of the renewable energy source are the same as that of scheme 1, which has been shown in Fig. 8. Then, the system simulation waveform is shown in Fig. 13.

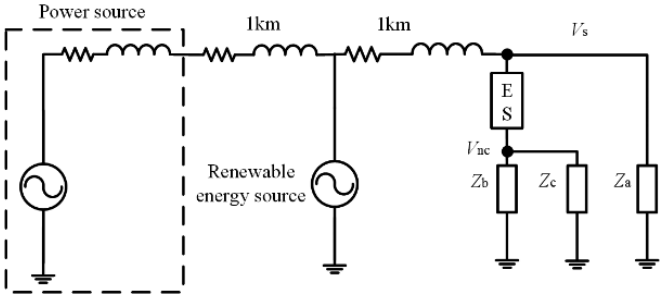

Fig. 12. System diagram of scheme 3

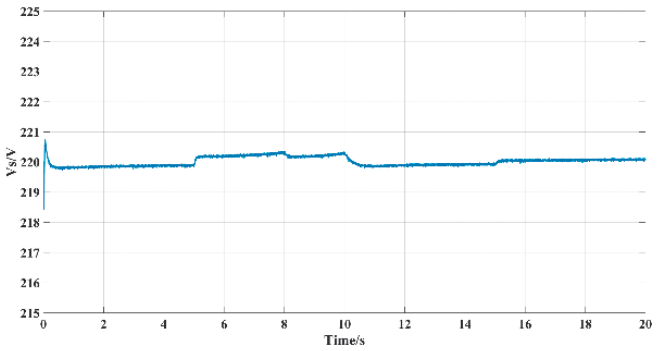

(a)

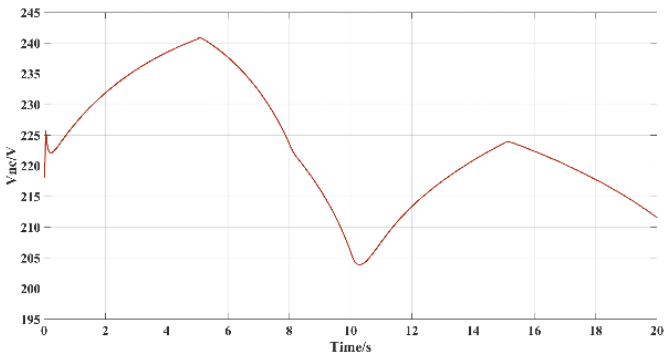

(b)

Fig. 13. System simulation waveform of scheme 3: system voltage V_{s} (a); noncritical load voltage V_{nc} (b)

As can be seen from Fig. 13(a), when loads b and c are connected in series with the ES as noncritical loads, the adjustment capability of the ES is significantly improved compared with the scheme 2. The maximum deviation of the system voltage V_s is only 0.3 V (+0.14%), which ensures the reliable operation of critical load a. However, as shown in Fig. 13(b), the maximum value of the noncritical load voltage is 240.9 V (+9.5%) and the minimum value is 203.8 V (−7.4%), which cannot satisfy the requirement of the voltage excursion of load b (allowable voltage excursion range is 7%). As a result, load b cannot work properly while becoming noncritical load, and may reduce the service life of load b. So this scheme cannot meet the needs of the user.

Scheme 4: The ES is connected to the system. Set load a as a critical load, load b as the class A noncritical load, and load c as the class B noncritical load.

The corresponding system diagram of scheme 4 is shown in Fig. 14. ES2, which is in series with the class B noncritical load, is a conventional ES ($V_{\text{dc-ref}} = 400$ V). As the allowable excursion range of load b is $a\% = 7\%$, the corresponding $V_{\text{es max}}$ is 43.3 V and 31.2 V respectively, which can be calculated by (6) and (11). So to ensure that the voltage excursion range of V_{nc1} is no more than 7%, $V_{\text{es max}}$ takes the smaller value, that is, $V_{\text{es max}} = 31.2$ V. Thus, the reference voltage at DC side of ES1 is 88.25 V which can be calculated by (13). ES1 and ES2 start at $t = 0$ s at the same time, the changes of the reactive power of the renewable energy resource are the same as that of scheme 1, which has been shown in Fig. 8. The simulation waveform of the system is shown in Fig. 15.

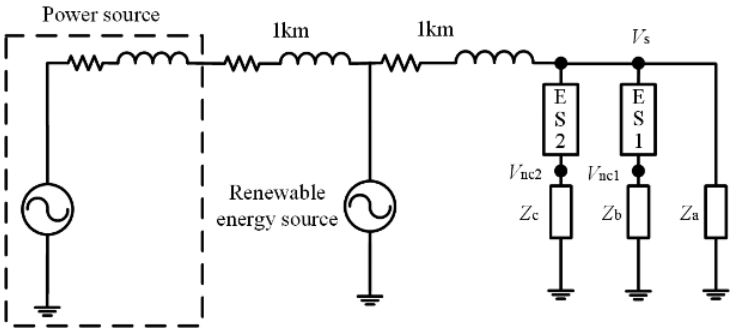

Fig. 14. Sstem diagram of scheme 4

As can be seen from Fig. 15(a), when the noncritical load is in series with the ES after being classified, the stability of the system voltage V_s can be effectively ensured (the maximum deviation of V_s is 0.18%) and the load a can work reliably. It can be seen from Fig. 15(b) that the maximum voltage excursion of the class A noncritical loads is 234.8 V and the minimum value is 209.3 V, the excursion ranges are +6.7% and −4.9% respectively, which can meet the requirement that the voltage excursion of load b is no more than 7%. Thus, load b can work normally. This scheme verifies the feasibility and effectiveness of the ES voltage stable control method proposed in this paper considering noncritical load voltage constraint.

Comparing scheme 4 with schemes 1–3, it can be found that scheme 4 can guarantee the stability and reliability of system voltage V_s, and meets the requirements of operating voltage

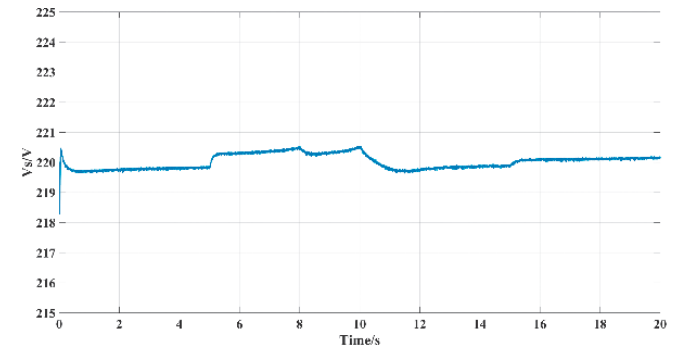

(a)

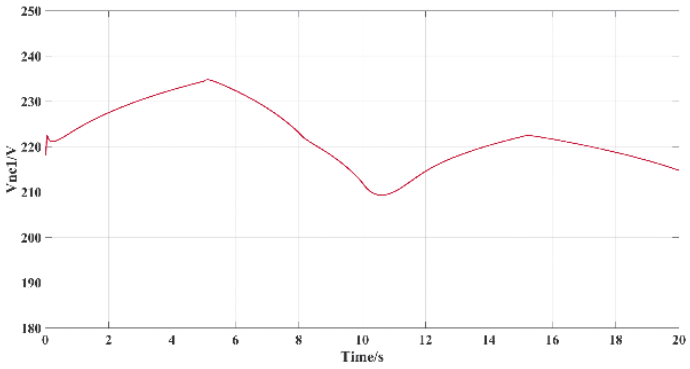

(b)

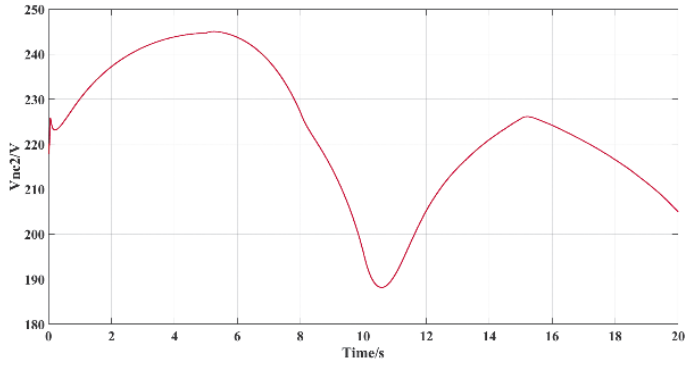

(c)

Fig. 15. System simulation waveform of scheme 4: system voltage V_s (a); class A noncritical load voltage V_{nc1} (b); class B noncritical load voltage V_{nc2} (c)

excursion of load b. Therefore, more kinds of loads can be used as the class A noncritical load to be connected to the system without affecting its normal operation, which helps to improve the ES voltage stable control ability.

5. Conclusion

This paper fully considers the operating voltage requirement of the noncritical load. Firstly, we classify the noncritical load, and comprehensively analyze the working phasor diagram of the ES under different types of loads (resistive load, resistive-inductive load). Then, we propose the ES control method considering the noncritical load voltage constraints, which can realize the limitation of voltage excursion of the class A noncritical load and meet the preset voltage range of the class A noncritical load. As a result, the access types of noncritical load can be increased and the voltage stable control ability of the ES can be improved effectively.

It can be seen from the simulation results that:

(1) The proposed ES control method considering noncritical load constraint can effectively ensure that the voltage of the class A noncritical load meets the requirements of normal operation. (2) By classifying noncritical loads, the types of load connected to the system can be effectively increased. So, more types of loads can participate in the voltage stable control of the ES as noncritical loads to improve the performance. (3) Reasonable ES access can effectively ensure the stability and reliability of the system voltage. However, since the majority of loads are resistive or resistive-inductive loads, this paper does not consider resistive-capacitive load. Also, the simulation environment is relatively simple and lack of practical experiments. In the future, more examples should be conduct to verify the proposed method further, and the realistic experiment model should be established to conduct the verification.

Acknowledgements

This work was supported by NSF of China (51607093), NSF of Jiangsu Province (BK2014 1452), Program of Natural Science Research of Jiangsu Higher Education Institutions of China (14KJB470006).

References

[1] Ma G., Xu G.C., Chen Y.X., Ju R., *Multi-objective optimal configuration method for a standalone wind–solar–battery hybrid power system*, IET Renewable Power Generation, vol. 11, no. 1, pp. 194–202 (2017).

[2] Yazdanian M., Mehrizi-Sani A., *Distributed Control Techniques in Microgrids*, IEEE Transactions on Smart Grid, vol. 5, no. 6, pp. 2901–2909 (2014).

[3] Aslani A., Helo P., Naaranoja M., *Evaluation of renewable energy development in power generation in Finland*, Journal of Renewable and Sustainable Energy, vol. 5, no. 6, pp. 1–13 (2013).

[4] Zhao S.S., Sheng W.X., Meng X.L., Song X.H., *Multi-resolution Model and Methodology for Analyzing the Impact of Voltage Quality on Maximum Penetration Level of Distributed Generation*, Proceedings of CSEE, vol. 35, no. 6, pp. 1306–1313 (2015).

[5] Abapour S., Zare K., Mohammadi-Ivatloo B., *Dynamic planning of distributed generation units in active distribution network*, IET Generation, Transmission and Distribution, vol. 9, no. 12, pp. 1455–1463 (2015).

[6] Wang C.M., Sun W.Q., Yi T., Yan Z.M., Zhang Y., *Review on Energy Storage Application Planning and Benefit Evaluation Methods in Smart Grid*, Proceedings of CSEE, vol. 33, no. 7, pp. 33–41 (2013).

[7] Luo X., Akhtar Z., Lee C.K., Chaudhuri B., Tan S.C., Hui S.Y.R., *Distributed Voltage Control with Electric Springs: Comparison with STATCOM*, IEEE Transactions on Smart Grid, vol. 6, no. 1, pp. 209–219 (2015).

[8] Hui S.Y., Lee C.K., Wu F.F., *Electric Springs – A New Smart Grid Technology*, IEEE Transactions Smart Grid, vol. 3, no. 3, pp. 1552–1561 (2012).

[9] Lee C.K., Hui S.Y.R., *Reduction of Energy Storage Requirements in Future Smart Grid Using Electric Springs*, IEEE Transactions on Smart Grid, vol. 4, no. 3, pp. 1282–1288 (2013).

[10] Chaudhuri N.R., Lee C.K., Chaudhuri B., Hui S.Y.R., *Dynamic Modeling of Electric Springs*, IEEE Transactions on Smart Grid, vol. 5, no. 5, pp. 2450–2458 (2014).

[11] Lee C.K., Chaudhuri N.R., Chaudhuri B., Hui S.Y.R., *Droop Control of Distributed Electric Springs for Stabilizing Future Power Grid*, IEEE Transactions on Smart Grid, vol. 4, no. 3, pp. 1558−1566 (2013).

[12] Cheng M, Wang Q.S., Zhang J.Z., *Theoretical Analysis and Controller Design of Electric Springs*, Proceedings of CSEE. vol. 35, no. 10, pp. 2436-2444 (2015).

[13] Lee C.K., Chaudhuri B., Hui S.Y., *Hardware and Control Implementation of Electric Springs for Stabilizing Future Smart Grid With Intermittent Renewable Energy Sources*, IEEE Journal of Emerging and Selected Topics in Power Electronics, vol. 1, no. 1, pp. 18–27 (2013).

[14] Wang Q., Cheng M., Chen Z., *Steady-State Analysis of Electric Springs With a Novel δ Control*, IEEE Transactions on Power Electronics, vol. 30, no. 12, pp. 7159–7169 (2015).

[15] Chen X., Hou Y., Tan S.C., Lee C.K., Hui S.Y.R., *Mitigating Voltage and Frequency Fluctuation in Microgrids Using Electric Springs*, IEEE Transactions on Smart Grid, vol. 6, no. 2, pp. 508–515 (2015).

[16] Zhao C.H., Ju R., Wu H.X., *Power Supply and Distribution System*, China Electric Power Press (2009).